

Modelling of FAST equilibrium configurations by a Toroidal Multipolar Expansion code using Kepler workflows

G Calabrò¹, E Giovannozzi¹, G Ramogida¹, F Crisanti¹, C Labate², M Mattei², P Micozzi¹ and G Vlad¹

¹ Associazione Euratom – ENEA sulla Fusione, Via Enrico Fermi 45, I-00044, Frascati (RM), Italy

² Associazione Euratom – ENEA – CREATE, Università di Napoli Federico II – Seconda Università di Napoli – Università di Reggio Calabria, Via Claudio 21, I-80125, Napoli, Italy

Fusion Advanced Studies Torus (FAST) has been proposed as a possible option for a European ITER Satellite facility, aimed at supporting the preparation of ITER operation scenarios and the exploration of technologies relevant to DEMO physics and technology issues in a wider (dimensionless) parameter space than JT-60SA and with characteristic values closer to ITER. FAST equilibrium configurations were designed in order to reproduce those of ITER with scaled plasma current. These equilibria, suitable to fulfil plasma conditions of relevance for studying integrated burning plasma physics, have been calculated using FIXFREE, a FORTRAN toroidal multipolar expansions equilibrium code, developed in Frascati and recently ported to the Integrated Tokamak Modelling (ITM) Gateway platform.

The European ITM Task Force opted for the open source workflow system Kepler to link various codes (actors) and coordinate the data flow among them. These actors are independent of a particular device and interact with each other via consistent physical objects (CPOs), i.e. data structures containing all relevant information on machine description and plasma parameters. In order to design the FAST equilibria, the FIXFREE code has been modified to be run as an actor in the Kepler environment. The configurations for FAST H-mode and Advanced Tokamak scenarios are presented.

FAST MACHINE DESIGN

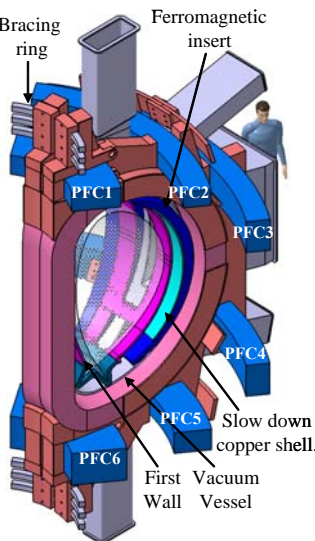
The design is based on a compact, high toroidal field tokamak able to operate in a wide range of plasma scenarios from the high performance H-Mode (B_T up to 8.5 T, I_p up to 8 MA) to the Advanced Tokamak operation (I_p up to 3 MA, not inductive current ratio up to 100%, pulse duration up to 160 s).

The toroidal field in FAST is produced by 18 Toroidal Field copper coils, cooled by 30 K Helium gas. This configuration will permit to place a NNBI heating system and a quantity of diagnostic measurements in the machine. The Poloidal Field System is made up of 6 Central Solenoid and 6 External copper coils, cooled by 30 K Helium gas.

The Vacuum Vessel is made of Inconel 625 and houses a First Wall comprising a bundle of water cooled tubes armored with plasma-sprayed Tungsten and an actively cooled divertor based on the hot radial pressing Tungsten monoblock tiles technology, which has been developed in ENEA and successfully tested up to 35 MW/m² heat flux.

The additional heating and Current Drive (CD) is provided by several systems:
 > Ion Cyclotron Resonance Heating (ICRH), 30 MW used as main radio-frequency heating system and to bring a large fraction of the minority species to very high energy in order to make it possible to investigate energetic particle physics in conditions to those of burning plasma;
 > Lower Hybrid (LH), 6 MW used for CD in the AT scenarios and to control the current profiles;

> Electron Cyclotron Resonance Heating (ECRH), 4 MW used for MHD control and for electrons heating and CD at lower densities;
 > Negative Neutral Beam Injection (NNBI), additional system up to 10 MW.

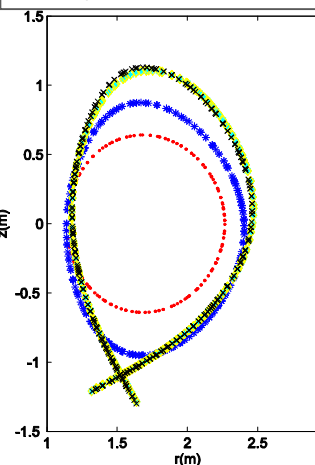


FAST EQUILIBRIUM CONFIGURATIONS

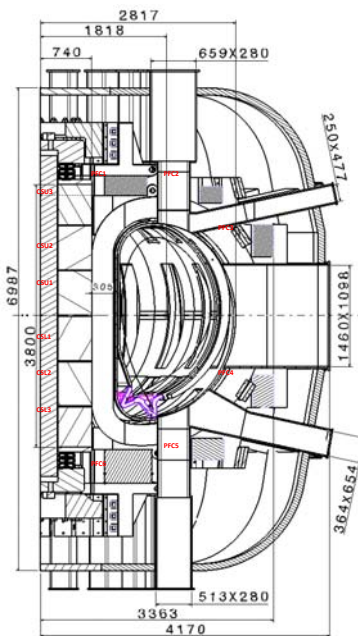
FAST equilibrium configurations have been designed to reproduce the physics of ITER relevant plasmas with scaled plasma current and to fulfil the conditions required to study, in an integrated framework, operation problems, plasma wall interactions and burning plasma physics issues. Main features are:

- (1) Plasma current, I_p , from 2 MA (corresponding to full NICD) up to 8 MA (corresponding to maximum performance);
- (2) Auxiliary heating systems able to accelerate the plasma ions to energies in the 0.5–1 MeV range;
- (3) Plasma major radius ≈ 1.8 m and minor radius around 0.65 m;
- (4) Pulse duration from 20 s for the reference H-mode scenario up to 160 s (~ 40 resistive times τ_{res}) in the AT 3 MA/3.5 T scenario.

FAST	H-mode referenc e	H-mode extreme	Hybrid	AT	AT2	AT Full NICD
I_p (MA)	6.5	8	5	3	3	2
q_{95}	3	2.6	4	5	3	5
B_T (T)	7.5	8.5	7.5	6	3.5	3.5
H_{95}	1	1	1.3	1.5	1.5	1.5
$\langle n_{95} \rangle$ (m ⁻³)	2	5	3	1.2	1.1	1
P_{th} (MW)	14 ÷ 18	22 ÷ 35	18 ÷ 23	8.5 ÷ 12	8.5 ÷ 12	5 ÷ 7
β_{95}	1.3	1.8	2.0	1.9	3.2	3.4
τ_E (s)	0.4	0.65	0.5	0.25	0.18	0.13
τ_{res} (s)	5.5	5	3	3	5 ÷ 6	2 ÷ 5
T_e (keV)	13.0	9.0	8.5	13	13	7.5
Q	0.65	2.5	0.9	0.19	0.14	0.06
$t_{discharge}$ (s)	20	10	20	70	170	140
$t_{heat-top}$ (s)	13	2	15	60	160	130
I_{NBI}/I_p (%)	15	15	30	60	80	100
p_{heat} (MW)	30	40	30	30	40	40
$p_{heat-ICRH}$ (MW)	30	30	30	30	30	30
$p_{heat-LH}$ (MW)	0	0	0	0	6	6
$p_{heat-ECRH}$ (MW)	0	0	0	0	4	4
$p_{heat-NNBI}$ (MW)	-	10	-	-	-	-



All the scenarios have same geometrical plasma features dictated by ITER similarity ($R_0=1.82m$, $a=0.64m$, $k=1.7$, $\langle \delta \rangle > 0.4$) and guarantee a minimum distance greater than 3 cm between the plasma last closed magnetic surface and the FW, to minimize their interaction (the power flux e-folding length λ_p has been assumed to be 0.5–1.0 cm on the outer equatorial plane).



The main parameters of the reference H-mode equilibrium obtained by the ITM version FIXFREE code are in good agreement with those obtained by means of CREATE-NL and MAXFEA.

The time evolution of plasma boundary shape is essentially the same for both H-mode and AT scenarios, whereas the pressure profile is peaked ($\langle P \rangle / \langle P_0 \rangle = 3.5$) and the q profile is assumed to be slightly reversed, with $q_{axis} > 2$ and $q_{min} < 2$ (at around half radius) as expected.

The FIXFREE equilibrium configurations have been used to carry out transport simulations by means of JETTO (P1.1007, EPS 2010) and CRONOS (P5.142, EPS 2010) codes. The next stage of ITM FIXFREE further development will be its coupling to the European Transport Solver (ETS) within the Kepler workflow system. FIXFREE then may become one of the reference free-boundary equilibrium codes for the ITM.

FIXFREE CODE AND THE GRAD-SHAFRANOV EQUATION

The FIXFREE equilibrium code solves the Grad-Shafranov equation by using the semi-analytical expansion of the scalar flux function ψ in terms of toroidal multipoles based on the full toroidal coordinates. The equilibrium is solved iteratively, using an integration mesh with a circular cross section, both for free and fixed conditions. The data - i.e. currents in the external poloidal circuits, toroidal plasma current I_p , poloidal β_p and functional forms of the kinetic plasma pressure $P(\psi)$ and of the diamagnetic total plasma current $I^2(\psi)$ - are easily interpreted in terms of toroidal multipoles. The semi-analytical method makes the code extremely flexible in modifying the geometry because the dependence on the integration mesh is extremely reduced with respect to other fully numerical solution methods.

$$J_\phi(R, \psi) = 2\pi R \frac{d\psi(\psi)}{d\psi} + \frac{\mu_0}{4\pi R} \frac{dI^2(\psi)}{d\psi}$$

The Grad-Shafranov equation describes the plasma force balance in terms of the magnetic scalar flux function ψ which can be expanded in a series of toroidal multi-poles, by using the toroidal coordinate system. In this equilibrium equation $p(\psi)$ is the kinetic plasma pressure function and $I(\psi)$ is the diamagnetic plasma current function.

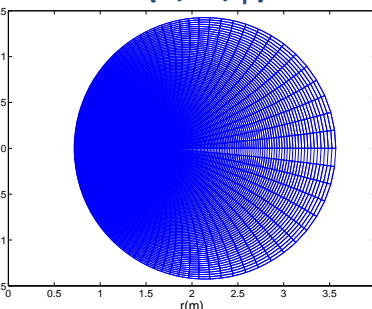
$$\psi = \frac{1}{\sqrt{\cosh\theta - \cos\omega}} \times \sum_{m=0}^{\infty} [M_m^i f_m(\cosh\theta) + M_m^e g_m(\cosh\theta)] \cos(m\omega) + C$$

- > Outside the plasma M_m^i and M_m^e are constants and depend on the conditions at the boundary of the domain.
- > Inside the plasma; $M_m^i(\theta)$ and $M_m^e(\theta)$ are internal and external multi-polar moments of order $m=1,2,\dots$ of the toroidal current density J_ϕ .
- > In the explicit expression of the internal and external moments $J_\phi(\theta_0, \omega_0)$ is the current density, δ_{m0} is the Kronecker's symbol, f_m and g_m are Fock's functions given in terms of half integer order, first degree Legendre functions of the first and second kinds.

$$M_m^i(\theta) = \frac{\mu_0 R_0^3 (2 - \delta_{m0})}{(m^2 - 1/4)} \times \int_0^{2\pi} \int_0^\theta J_\phi(\theta_0, \omega_0) \frac{g_m(\cosh\theta_0) \cos(m\omega_0)}{(\cosh\theta_0 - \cos\omega_0)^{5/2}} d\omega_0 d\theta_0$$

$$M_m^e(\theta) = \frac{\mu_0 R_0^3 (2 - \delta_{m0})}{(m^2 - 1/4)} \times \int_0^{2\pi} \int_0^\theta J_\phi(\theta_0, \omega_0) \frac{f_m(\cosh\theta_0) \cos(m\omega_0)}{(\cosh\theta_0 - \cos\omega_0)^{5/2}} d\omega_0 d\theta_0$$

TOROIDAL COORDINATE SYSTEM (θ, ω, ϕ)



The coordinate θ defines circular cross-section non-concentric with major and minor radii $R(\theta) = R_0 \cosh\theta$, $a(\theta) = R_0 / \sinh\theta$. The coordinate ω defines the spheres passing through the pole $R-R_0$ and has the simple meaning of a poloidal angle. (R, Z, Φ) is the cylindrical coordinate system.

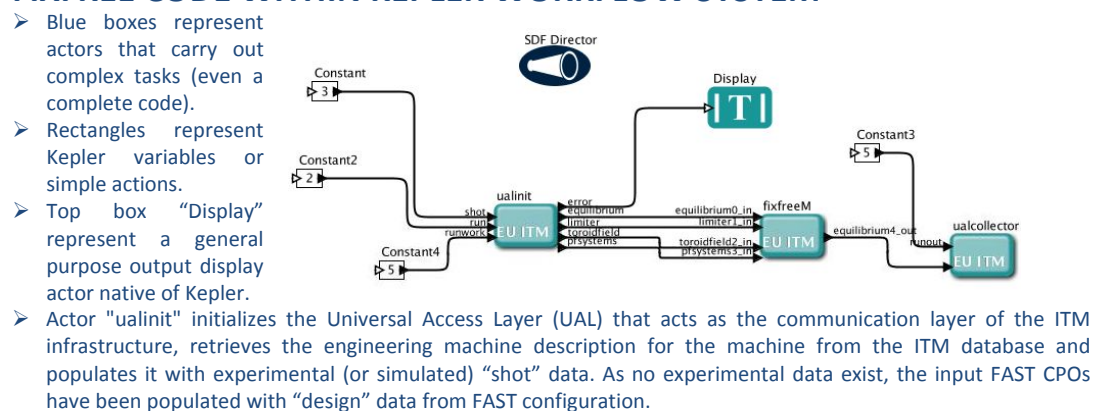
$$R = \frac{R_0 \sinh\theta}{\cosh\theta - \cos\omega} \quad Z = \frac{R_0 \sin\omega}{\cosh\theta - \cos\omega} \quad [0 < \theta < \infty \quad 0 < \omega < 2\pi]$$

MAIN INPUT-OUTPUT VARIABLES

Variable	Unit	Description
psi1	V	Poloidal flux (Wb), without 1/2pi and such that Bp = grad psi (1/2pi R)
psi2	V	Toroidal flux (Wb)
psi3	V	psi derivative (k Bphi) (T m)
p_dis	P	discharge pressure (Pa)
p_der	P	psi derivative of the pressure profile (Pa/Wb)
p_der2	P	psi derivative of p_dis multiplied with F_sln (T^2 m^2/Wb)
f_der	V	psi derivative of F_sln (T^2 m^2/Wb)
rho1	kg/m3	rho surface averaged toroidal current density = averaged (rho R) over (1/4pi R^2)
rho1_der	kg/m3	rho surface averaged toroidal current density averaged (rho R) over (1/4pi R^2)
rho1_der2	kg/m3	rho surface averaged toroidal current density averaged (rho R) over (1/4pi R^2)
rho1_der3	kg/m3	rho surface averaged toroidal current density averaged (rho R) over (1/4pi R^2)
rho1_der4	kg/m3	rho surface averaged toroidal current density averaged (rho R) over (1/4pi R^2)
rho1_der5	kg/m3	rho surface averaged toroidal current density averaged (rho R) over (1/4pi R^2)
rho1_der6	kg/m3	rho surface averaged toroidal current density averaged (rho R) over (1/4pi R^2)
rho1_der7	kg/m3	rho surface averaged toroidal current density averaged (rho R) over (1/4pi R^2)
rho1_der8	kg/m3	rho surface averaged toroidal current density averaged (rho R) over (1/4pi R^2)
rho1_der9	kg/m3	rho surface averaged toroidal current density averaged (rho R) over (1/4pi R^2)
rho1_der10	kg/m3	rho surface averaged toroidal current density averaged (rho R) over (1/4pi R^2)
rho1_der11	kg/m3	rho surface averaged toroidal current density averaged (rho R) over (1/4pi R^2)
rho1_der12	kg/m3	rho surface averaged toroidal current density averaged (rho R) over (1/4pi R^2)
rho1_der13	kg/m3	rho surface averaged toroidal current density averaged (rho R) over (1/4pi R^2)
rho1_der14	kg/m3	rho surface averaged toroidal current density averaged (rho R) over (1/4pi R^2)
rho1_der15	kg/m3	rho surface averaged toroidal current density averaged (rho R) over (1/4pi R^2)
rho1_der16	kg/m3	rho surface averaged toroidal current density averaged (rho R) over (1/4pi R^2)
rho1_der17	kg/m3	rho surface averaged toroidal current density averaged (rho R) over (1/4pi R^2)
rho1_der18	kg/m3	rho surface averaged toroidal current density averaged (rho R) over (1/4pi R^2)
rho1_der19	kg/m3	rho surface averaged toroidal current density averaged (rho R) over (1/4pi R^2)
rho1_der20	kg/m3	rho surface averaged toroidal current density averaged (rho R) over (1/4pi R^2)
rho1_der21	kg/m3	rho surface averaged toroidal current density averaged (rho R) over (1/4pi R^2)
rho1_der22	kg/m3	rho surface averaged toroidal current density averaged (rho R) over (1/4pi R^2)
rho1_der23	kg/m3	rho surface averaged toroidal current density averaged (rho R) over (1/4pi R^2)
rho1_der24	kg/m3	rho surface averaged toroidal current density averaged (rho R) over (1/4pi R^2)
rho1_der25	kg/m3	rho surface averaged toroidal current density averaged (rho R) over (1/4pi R^2)
rho1_der26	kg/m3	rho surface averaged toroidal current density averaged (rho R) over (1/4pi R^2)
rho1_der27	kg/m3	rho surface averaged toroidal current density averaged (rho R) over (1/4pi R^2)
rho1_der28	kg/m3	rho surface averaged toroidal current density averaged (rho R) over (1/4pi R^2)
rho1_der29	kg/m3	rho surface averaged toroidal current density averaged (rho R) over (1/4pi R^2)
rho1_der30	kg/m3	rho surface averaged toroidal current density averaged (rho R) over (1/4pi R^2)
rho1_der31	kg/m3	rho surface averaged toroidal current density averaged (rho R) over (1/4pi R^2)
rho1_der32	kg/m3	rho surface averaged toroidal current density averaged (rho R) over (1/4pi R^2)
rho1_der33	kg/m3	rho surface averaged toroidal current density averaged (rho R) over (1/4pi R^2)
rho1_der34	kg/m3	rho surface averaged toroidal current density averaged (rho R) over (1/4pi R^2)
rho1_der35	kg/m3	rho surface averaged toroidal current density averaged (rho R) over (1/4pi R^2)
rho1_der36	kg/m3	rho surface averaged toroidal current density averaged (rho R) over (1/4pi R^2)
rho1_der37	kg/m3	rho surface averaged toroidal current density averaged (rho R) over (1/4pi R^2)
rho1_der38	kg/m3	rho surface averaged toroidal current density averaged (rho R) over (1/4pi R^2)
rho1_der39	kg/m3	rho surface averaged toroidal current density averaged (rho R) over (1/4pi R^2)
rho1_der40	kg/m3	rho surface averaged toroidal current density averaged (rho R) over (1/4pi R^2)
rho1_der41	kg/m3	rho surface averaged toroidal current density averaged (rho R) over (1/4pi R^2)
rho1_der42	kg/m3	rho surface averaged toroidal current density averaged (rho R) over (1/4pi R^2)
rho1_der43	kg/m3	rho surface averaged toroidal current density averaged (rho R) over (1/4pi R^2)
rho1_der44	kg/m3	rho surface averaged toroidal current density averaged (rho R) over (1/4pi R^2)
rho1_der45	kg/m3	rho surface averaged toroidal current density averaged (rho R) over (1/4pi R^2)
rho1_der46	kg/m3	rho surface averaged toroidal current density averaged (rho R) over (1/4pi R^2)
rho1_der47	kg/m3	rho surface averaged toroidal current density averaged (rho R) over (1/4pi R^2)
rho1_der48	kg/m3	rho surface averaged toroidal current density averaged (rho R) over (1/4pi R^2)
rho1_der49	kg/m3	rho surface averaged toroidal current density averaged (rho R) over (1/4pi R^2)
rho1_der50	kg/m3	rho surface averaged toroidal current density averaged (rho R) over (1/4pi R^2)
rho1_der51	kg/m3	rho surface averaged toroidal current density averaged (rho R) over (1/4pi R^2)
rho1_der52	kg/m3	rho surface averaged toroidal current density averaged (rho R) over (1/4pi R^2)
rho1_der53	kg/m3	rho surface averaged toroidal current density averaged (rho R) over (1/4pi R^2)
rho1_der54	kg/m3	rho surface averaged toroidal current density averaged (rho R) over (1/4pi R^2)
rho1_der55	kg/m3	rho surface averaged toroidal current density averaged (rho R) over (1/4pi R^2)
rho1_der56	kg/m3	rho surface averaged toroidal current density averaged (rho R) over (1/4pi R^2)
rho1_der57	kg/m3	rho surface averaged toroidal current density averaged (rho R) over (1/4pi R^2)
rho1_der58	kg/m3	rho surface averaged toroidal current density averaged (rho R) over (1/4pi R^2)
rho1_der59	kg/m3	rho surface averaged toroidal current density averaged (rho R) over (1/4pi R^2)
rho1_der60	kg/m3	rho surface averaged toroidal current density averaged (rho R) over (1/4pi R^2)
rho1_der61	kg/m3	rho surface averaged toroidal current density averaged (rho R) over (1/4pi R^2)
rho1_der62	kg/m3	rho surface averaged toroidal current density averaged (rho R) over (1/4pi R^2)
rho1_der63	kg/m3	rho surface averaged toroidal current density averaged (rho R) over (1/4pi R^2)
rho1_der64	kg/m3	rho surface averaged toroidal current density averaged (rho R) over (1/4pi R^2)
rho1_der65	kg/m3	rho surface averaged toroidal current density averaged (rho R) over (1/4pi R^2)
rho1_der66	kg/m3	rho surface averaged toroidal current density averaged (rho R) over (1/4pi R^2)
rho1_der67	kg/m3	rho surface averaged toroidal current density averaged (rho R) over (1/4pi R^2)
rho1_der68	kg/m3	rho surface averaged toroidal current density averaged (rho R) over (1/4pi R^2)
rho1_der69	kg/m3	rho surface averaged toroidal current density averaged (rho R) over (1/4pi R^2)
rho1_der70	kg/m3	rho surface averaged toroidal current density averaged (rho R) over (1/4pi R^2)
rho1_der71	kg/m3	rho surface averaged toroidal current density averaged (rho R) over (1/4pi R^2)
rho1_der72	kg/m3	rho surface averaged toroidal current density averaged (rho R) over (1/4pi R^2)
rho1_der73	kg/m3	rho surface averaged toroidal current density averaged (rho R) over (1/4pi R^2)
rho1_der74	kg/m3	rho surface averaged toroidal current density averaged (rho R) over (1/4pi R^2)
rho1_der75	kg/m3	rho surface averaged toroidal current density averaged (rho R) over (1/4pi R^2)
rho1_der76	kg/m3	rho surface averaged toroidal current density averaged (rho R) over (1/4pi R^2)
rho1_der77	kg/m3	rho surface averaged toroidal current density averaged (rho R) over (1/4pi R^2)
rho1_der78	kg/m3	rho surface averaged toroidal current density averaged (rho R) over (1/4pi R^2)
rho1_der79	kg/m3	rho surface averaged toroidal current density averaged (rho R) over (1/4pi R^2)
rho1_der80	kg/m3	rho surface averaged toroidal current density averaged (rho R) over (1/4pi R^2)
rho1_der81	kg/m3	rho surface averaged toroidal current density averaged (rho R) over (1/4pi R^2)
rho1_der82	kg/m3	rho surface averaged toroidal current density averaged (rho R) over (1/4pi R^2)
rho1_der83	kg/m3	rho surface averaged toroidal current density averaged (rho R) over (1/4pi R^2)
rho1_der84	kg/m3	rho surface averaged toroidal current density averaged (rho R) over (1/4pi R^2)
rho1_der85	kg/m3	rho surface averaged toroidal current density averaged (rho R) over (1/4pi R^2)
rho1_der86	kg/m3	rho surface averaged toroidal current density averaged (rho R) over (1/4pi R^2)
rho1_der87	kg/m3	rho surface averaged toroidal current density averaged (rho R) over (1/4pi R^2)
rho1_der88	kg/m3	rho surface averaged toroidal current density averaged (rho R) over (1/4pi R^2)
rho1_der89	kg/m3	rho surface averaged toroidal current density averaged (rho R) over (1/4pi R^2)
rho1_der90	kg/m3	rho surface averaged toroidal current density averaged (rho R) over (1/4pi R^2)
rho1_der91	kg/m3	rho surface averaged toroidal current density averaged (rho R) over (1/4pi R^2)
rho1_der92	kg/m3	rho surface averaged toroidal current density averaged (rho R) over (1/4pi R^2)
rho1_der93	kg/m3	rho surface averaged toroidal current density averaged (rho R) over (1/4pi R^2)
rho1_der94	kg/m3	rho surface averaged toroidal current density averaged (rho R) over (1/4pi R^2)
rho1_der95	kg/m3	rho surface averaged toroidal current density averaged (rho R) over (1/4pi R^2)
rho1_der96	kg/m3	rho surface averaged toroidal current density averaged (rho R) over (1/4pi R^2)
rho1_der97	kg/m3	rho surface averaged toroidal current density averaged (rho R) over (1/4pi R^2)
rho1_der98	kg/m3	rho surface averaged toroidal current density averaged (rho R) over (1/4pi R^2)
rho1_der99	kg/m3	rho surface averaged toroidal current density averaged (rho R) over (1/4pi R^2)
rho1_der100	kg/m3	rho surface averaged toroidal current density averaged (rho R) over (1/4pi R^2)

- > Some input parameters could be passed to FIXFREE through CPOs (basically the coil geometries and currents, magnetic field and plasma current), while others must be imported by XML files in the code-parameters section of the equilibrium CPO through a FORTRAN library, based on the open source XML2LIB library, which has been developed to parse and to interpret XML files.
- > To adapt FIXFREE to ITM requirements, some quantities have been added to the output variables respect to the original code and the description of the poloidal field coils (PFC) is now read from the PFSSYSTEM CPO instead of being specified together with other code parameters.
- > The structure of FIXFREE has also been modified to always run as a batch job instead of in an interactive way.
- > A program that populates MDSPLUS trees with the FAST data has also been written and finally all has been assembled within a Kepler actor.

FIXFREE CODE WITHIN KEPLER WORKFLOW SYSTEM



ACKNOWLEDGEMENT: This work, supported by the European Communities under the EURATOM/ENEA contract of Association, was carried out within the framework of the European Fusion Development Agreement. The views and opinions expressed herein do not necessarily reflect those of the European Commission.